ACS APPLIED MATERIALS & INTERFACES

Letter

www.acsami.org

Nanowires as Building Blocks to Fabricate Flexible Thermoelectric Fabric: The Case of Copper Telluride Nanowires

Chongjian Zhou,[†,‡] Chaochao Dun,[†,⊥] Qiong Wang,[‡] Ke Wang,[‡] Zhongqi Shi,[*,‡] David L. Carroll,[*,⊥] Guiwu Liu,[*,§] and Guanjun Qiao[‡,§]

[‡]State Key Laboratory for Mechanical Behavior of Materials, Xi'an Jiaotong University, Xi'an 710049, China

[§]School of Materials Science and Engineering, Jiangsu University, Zhenjiang 212013, China

[⊥]Center for Nanotechnology and Molecular Materials, Department of Physics, Wake Forest University, Winston-Salem, North Carolina 27109, United States

Supporting Information

ABSTRACT: A general approach to fabricate nanowires based inorganic/organic composite flexible thermoelectric fabric using a simple and efficacious five-step vacuum filtration process is proposed. As an excellent example, the performance of freestanding flexible thermoelectric thin film using copper telluride nanowires/polyvinylidene fluoride ($Cu_{1.75}Te$ NWs/PVDF = 2:1) as building block is demonstrated. By burying the $Cu_{1.75}Te$ NWs into the PVDF polymer agent, the flexible fabric exhibits room-temperature Seebeck coefficient and electric conductivity of 9.6 μV/K and 2490 S/cm, respectively, resulting in a power factor of 23 $\mu W/(mK^2)$ that is comparable to the bulk counterpart. Furthermore, this NW-based flexible fabric can endure hundreds of cycles of bending tests without significant performance degradation.

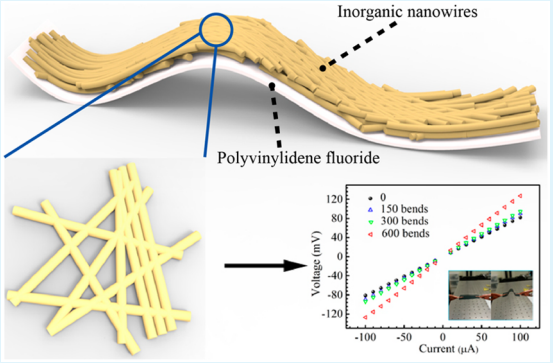

KEYWORDS: *thermoelectric, fabric, $Cu_{1.75}Te$ nanowire, organic−inorganic composite, flexibility*

Thermoelectric materials, which can directly convert heat to electric or vice versa, offer a promising potential to convert body heat continuously into electrical power that can be applied to portable/wearable electronic devices.[1,2] One of the most crucial factors for thermoelectric materials used in the portable devices is flexibility.[3] Unfortunately, the traditional inorganic bulk thermoelectric materials[4,5] are brittle and fragile, whereas organic flexible polymers often possess poor thermoelectric performance,[6] making them unsuitable for kinetic applications. Recently, with the reduction of dimensionality and size, inorganic materials would become flexible/plastic to a certain extent.[7] However, the flexibility of nanosized inorganic materials is too poor to fabricate freestanding thermoelectric fabrics by themselves.[3] Therefore, combining the flexible polymer with some kinds of inorganic nanomaterials that have great thermoelectric performance and a certain flexibility is regarded as an effective route to solve this predicament.[1,8−11]

Up to now, zero dimensional (0D) and two-dimensional (2D) nanostructures have been applied to fabricate flexible thermoelectric fabrics.[1,11−13] Normally, these nanostructures are dispersed in solutions to form stable and easy-to-handle colloidal inks, allowing solution processing of thermoelectric fabrics or fibers. So far, the most commonly used inorganic colloidal inks are 0D quantum dot materials,[14] which can readily form thermodynamically stable colloidal solutions and be further modulated into thin film materials on diverse substrates (such as nylon cloth[12] and glass fiber[13]) via a simple dip coating process. However, these thermoelectric fabrics are too vulnerable due to the weak bonding between the 0D nanocrystal and substrates. Moreover, the 0D nanocrystal coated flexible thermoelectric films possess low electric conductivity owing to the induced electron scattering caused by the large number of grain boundaries,[15] leading to low power factor eventually. Compared with the 0D nanocrystal, the 2D nanostructures were proved to be a better choice to manufacture organic/inorganic flexible thermoelectric fabrics to a certain extent because of the reduced grain boundaries and high surface coverage (~90%).[1,10] In our previous report,[1] the Bi_2Se_3 nanoplate/PVDF composite exhibits a power factor of near 30 $\mu W/(mK^2)$. However, according to the previous studies,[15] the electric conductivity of nanoplate is still lower than that of one-dimensional (1D) nanostructured counterpart. At this point, the 1D nanostructure based composite is believed to be another promising build block for thermoelectric fabrics.[16] To date, the most common inorganic materials to fabricate organic/inorganic fabrics are Te nanowires/nanorods.[2,8,17] Nevertheless, most of these fabrics are not highly flexible.[8,9] Moreover, few reports on the metal tellurides were

Received: August 4, 2015
Accepted: September 16, 2015
Published: September 16, 2015

DOI: 10.1021/acsami.5b07144
ACS Appl. Mater. Interfaces 2015, 7, 21015−21020

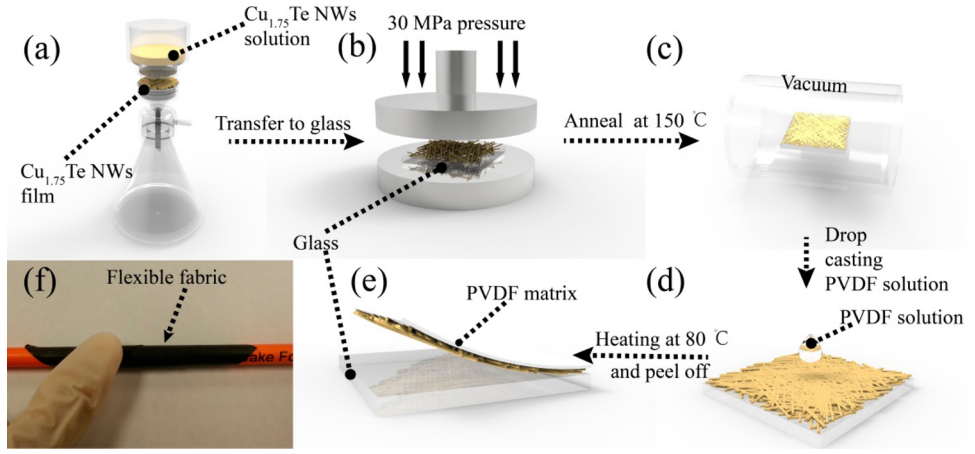

Figure 1. Schematic illustration of the fabrication procedure for the flexible thermoelectric fabric, including (a) vacuum filtration to form a NWs film, (b) mechanical pressing using a 30 MPa pressure for 15 s after cutting the film into square and transferring to a cleaning glass, (c) annealing at 150 °C in vacuum for 30 min, (d) drop-coating PVDF solution upon the film, and (e) peeling off the NWs/PVDF film by immersing the film in methanol after baking 2 h to evaporate DMF. (f) The roll-up photograph of the as-fabricated thermoelectric film demonstrates the highly flexibility.

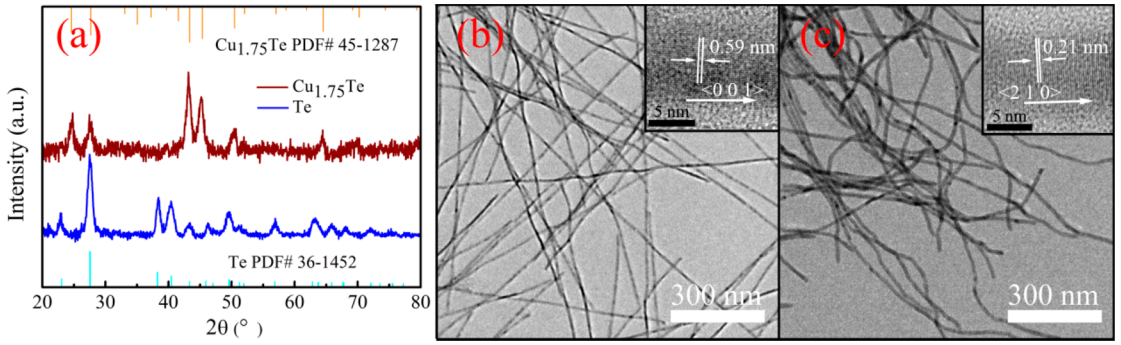

Figure 2. (a) XRD patterns of pristine Te (blue) and $Cu_{1.75}Te$ NWs (dark brown), the corresponding standard Te (cyan) and $Cu_{1.75}Te$ (orange) were also displayed; (b, c) TEM images with insets showing the corresponding HRTEM images of Te and $Cu_{1.75}Te$ NWs, respectively.

found, which actually possess promising thermoelectric performance and have been widely used in bulk thermoelectrics.

Herein, a general method to fabricate flexible organic/inorganic thermoelectric fabric by vacuum filtration using copper telluride nanowires ($Cu_{1.75}Te$ NWs) as building block and PVDF as flexible substrate is put forward. This 1D NW-based flexible thermoelectric fabric has the following merits: (I) the tightly connected 3D NW-based-network can enhance electrical conductivity of the composite film; (II) compared with the 0D quantum dot and 2D nanoplate based fabrics, the 1D NW-based fabric possess a higher surface coverage and thus higher durability, especially for the highly flexible $Cu_{1.75}Te$ NWs;[16] (III) the vacuum filtration route is easily scaled up for wide applications and can be extended to other inorganic NW-based fabrics.

The fabrication process of $Cu_{1.75}Te$ NWs/PVDF flexible thermoelectric fabric is divided into the following five steps: (I) synthesis of $Cu_{1.75}Te$ NWs with high aspect ratio and removal of surfactant surrounded the NWs;[18] (II) fabrication of the $Cu_{1.75}Te$ NWs film by vacuum filtration, and the fabricated thin film is cut into square and transferred to a cleaned glass substrate;[19] (III) the film on the glass substrate is compacted under a pressure of 30 MPa for 15 s, and then annealed at 150 °C in vacuum; (IV) proper amount of PVDF dissolved in dimethylformamide (DMF) is drop-coated on the $Cu_{1.75}Te$ NWs film and heated to 80 °C for holding 2 h to evaporate the DMF; (V) the film is peeled off by immersing in methanol to obtain the fabric. The detailed fabrication procedure is illustrated in Figure 1, with Figure 1f demonstrating the high flexibility of as-fabricated thermoelectric fabric. Experimental details are provided in Supporting Information. Here, considering the compromise between electrical conductivity and flexibility, $Cu_{1.75}Te$ NWs/PVDF fabrics with ratio of 2:1 is adopted, which has the optimized performance.

Figure 2 shows the X-ray diffraction (XRD) patterns and the corresponding transmission electron microscope (TEM) images of Te NWs and the subsequent copper telluride NWs. From the XRD pattern (Figure 2a), no impurities can be detected for copper telluride, suggesting that the as-synthesized Te NWs converted into copper telluride NWs completely. All the diffraction peaks are in great agreement with the copper telluride, which was further indexed to $Cu_{1.75}Te$ determined by EDS (Figure S1). The wirelike 1D nanostructure was confirmed by TEM (Figure 2b, c). Statistical analyses of the TEM image revealed that the as-synthesized Te NWs have average diameter and length of 7 ± 1 nm and ~5 μm, respectively. In detail, when the mild reducing agent (ascorbic acid) was injected into the mixture solution with Te NWs and Cu^{2+} ions, Cu^{2+} ions were reduced to Cu^{+}. Then the reduced Cu^{+} ions would induce a disproportional reaction on surface of Te NWs by Te → Te^{4+}+Te^{2-}. Finally, Cu^{+} ions reacted with Te^{2-} and in situ formed a stable copper poor stoichiometric structure $Cu_{1.75}Te$. The average diameter of the original

DOI: 10.1021/acsami.5b07144
ACS Appl. Mater. Interfaces 2015, 7, 21015−21020

nanowires increases to 10 ± 2 nm after Cu atoms were integrated into Te NWs and converted into $Cu_{1.75}Te$ NWs. It is worth mentioning that the $Cu_{1.75}Te$ NWs become curved along the axial direction, indicating the highly flexible nature.[20] Although the morphology of $Cu_{1.75}Te$ NWs made the accurate estimation of length impossible, it is obvious that the length increases more distinguishably than the diameter when the Te NWs are transformed into the $Cu_{1.75}Te$ NWs. This phenomenon is caused by the fact that both the Te and the $Cu_{1.75}Te$ possess hexagonal lattice structure, thus the transformation of lattice topology tends to be initiated along *c* axis, that is, the growth direction of Te NWs.

Before the $Cu_{1.75}Te$ NWs are annealed and buried upon PVDF, simple mechanical pressing as a preliminary treatment is necessary to reduce the number of junction,[21,22] because this strategy not only effectively increases the connection of $Cu_{1.75}Te$ NWs but also improves the film morphology. Specially, at the first beginning, the transferred $Cu_{1.75}Te$ NWs film deposited on the glass substrate is porous and poorly connected. As shown in Figure 1b, 30 MPa pressure was applied for 15 s on the $Cu_{1.75}Te$ NWs film, leading to a pretty tightly connected nanonetwork after the stamping process. However, there are still some weak connections among the $Cu_{1.75}Te$ NWs after stamping, which could reduce the electric conductivity significantly because of the carrier filtering effect at the interface. Therefore, the stamped $Cu_{1.75}Te$ NWs film is then annealed at 150 °C for 30 min in vacuum to allow the $Cu_{1.75}Te$ NWs melting and fusing at the junctions or along the axial direction. Finally, the $Cu_{1.75}Te$ NWs film is buried in the PVDF matrix by drop coating the PVDF solution.

From the top-viewed SEM image of the as-fabricated $Cu_{1.75}Te$/PVDF fabric, the unpressed fabric has a relatively rough surface (Figure 3a) and the $Cu_{1.75}Te$ NWs are loosely bounded (Figure 3b), which seriously deteriorated the electrical conductivity (~50 S/cm). On the contrary, the pressed and annealed fabric possesses a relatively smooth surface (Figure 3c), and all the $Cu_{1.75}Te$ NWs are tightly connected with each other (Figure 3d) with thickness around 5 μm. The after-treated fabric shows an improved electrical conductivity as high as ~2490 S/cm. The surface topographies of the as-fabricated $Cu_{1.75}Te$ NWs/PVDF fabric, examined by atomic force microscopy (AFM), are given in Figure 4. Figure 4a, c reveals a network of randomly oriented $Cu_{1.75}Te$ NWs before pressing, and the height elevation varies markedly (Figure 4b) with the average height around 40 nm. On the contrary, the surface topographies of the pressed and annealed fabric appears much smoother (in Figure 4d, f) and the average height variation of the 4 × 4 μm^2 scanning area is less than 20 nm (Figure 4e), which is much smaller than that of the unpressed one.

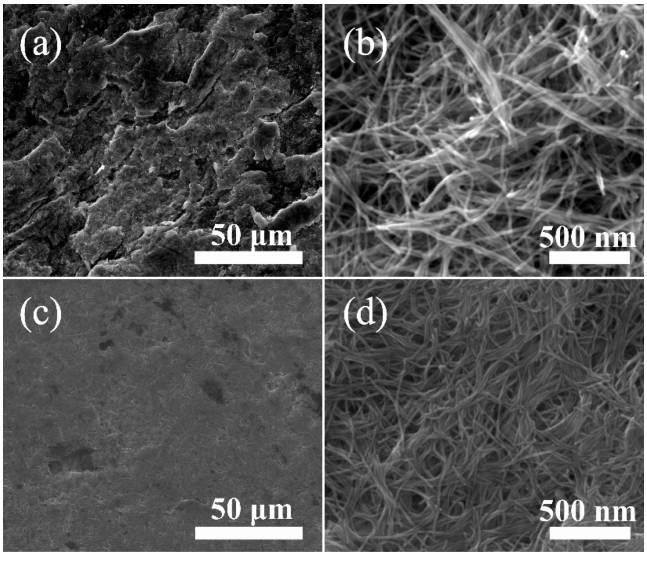

Figure 3. Top-viewed SEM images of the unpressed $Cu_{1.75}Te$ NWs/PVDF fabric with (a) low-resolution and (b) high-resolution, weak connection is clearly observed. (c, d) Corresponding SEM images of the after-treated $Cu_{1.75}Te$ NWs/PVDF fabric (pressed under 30 MPa and annealed at 150 °C in vacuum), revealing the tight connection.

For flexible thermoelectric fabrics, the thermoelectric property is normally evaluated by the so-called power factor ($PF = \alpha^2\sigma$), where α and σ are the Seebeck coefficient and electrical conductivity, respectively.[1,2] Here, the power factor of the as-prepared flexible $Cu_{1.75}Te$ NWs/PVDF fabric was measured using a custom built apparatus similar to that reported by Kim et al.[23] The measurement errors for the electrical conductivity and Seebeck coefficient were ±10 S/m and ±0.1 μV/K, respectively. Due to the ultralow conductivity of unpressed $Cu_{1.75}Te$ NWs/PVDF fabric, only the after-treated one is measured. The temperature-dependent electrical conductivity for the $Cu_{1.75}Te$ NWs/PVDF fabric is shown in Figure 5a. The room temperature value of 2490 S/cm is comparable to that of the Cu_2Te bulk counterpart.[24,25] It is noteworthy that the electrical conductivity of the after-treated $Cu_{1.75}Te$ NWs/PVDF fabric derived from the present fabrication process is about 60% of the reported values for the $Cu_{1.75}Te$ vacuum-deposited film counterpart,[26] whereas the simple mixture of the inorganic and PVDF only possess electrical conductivity about one-third of the bulk counterpart.[1] The enhancement of electrical conductivity can be attributed to the reduced grain boundaries after pressing and annealing. Meanwhile, the reduction in electrical conductivity (~40%) for the after-treated fabric compared with its bulk counterpart is mainly caused by the carrier scattering within the NW-NW junctions. Despite the slightly reduced conductivity by incorporation of NWs into the fabric, the temperature-dependent conductivity exhibits metallic behavior, which is exemplified by the negative slope with respect to temperature. This is in accordance with the previous report due to the high carrier concentrations accompanied by the large amount copper defects.[27] Metallic electrical conductivity is typically described by the Bloch−Gruneisen model, which is characterized by a near linear negative slop and low temperature leveling of conductivity because of a defect in the scattering residual resistivity.

The temperature dependence of the Seebeck coefficient for the $Cu_{1.75}Te$ NWs/PVDF fabric is shown Figure 5b. The positive slope indicates a majority of hole carriers. The exact room temperature value of 9.6 μV/K is slightly higher than that of the bulk counterpart,[25] which is mainly attributed to the NW's electron filtering effect at the interface. Because the carriers without sufficient energy are known to decrease the Seebeck coefficient, the enhancement of Seebeck coefficient for the after-treated fabric can be ascribed to the filtered carriers originated from the NW−NW conjunctions and the unconducting polymer PVDF. Although it was not shown here, it is observed that the Seebeck coefficient is exclusively determined by $Cu_{1.75}Te$ NWs without observable contribution from PVDF regardless with the ratio (see Figure S2). Furthermore, like our previous report,[1] the temperature-dependent Seebeck coef-

DOI: 10.1021/acsami.5b07144
ACS Appl. Mater. Interfaces 2015, 7, 21015−21020

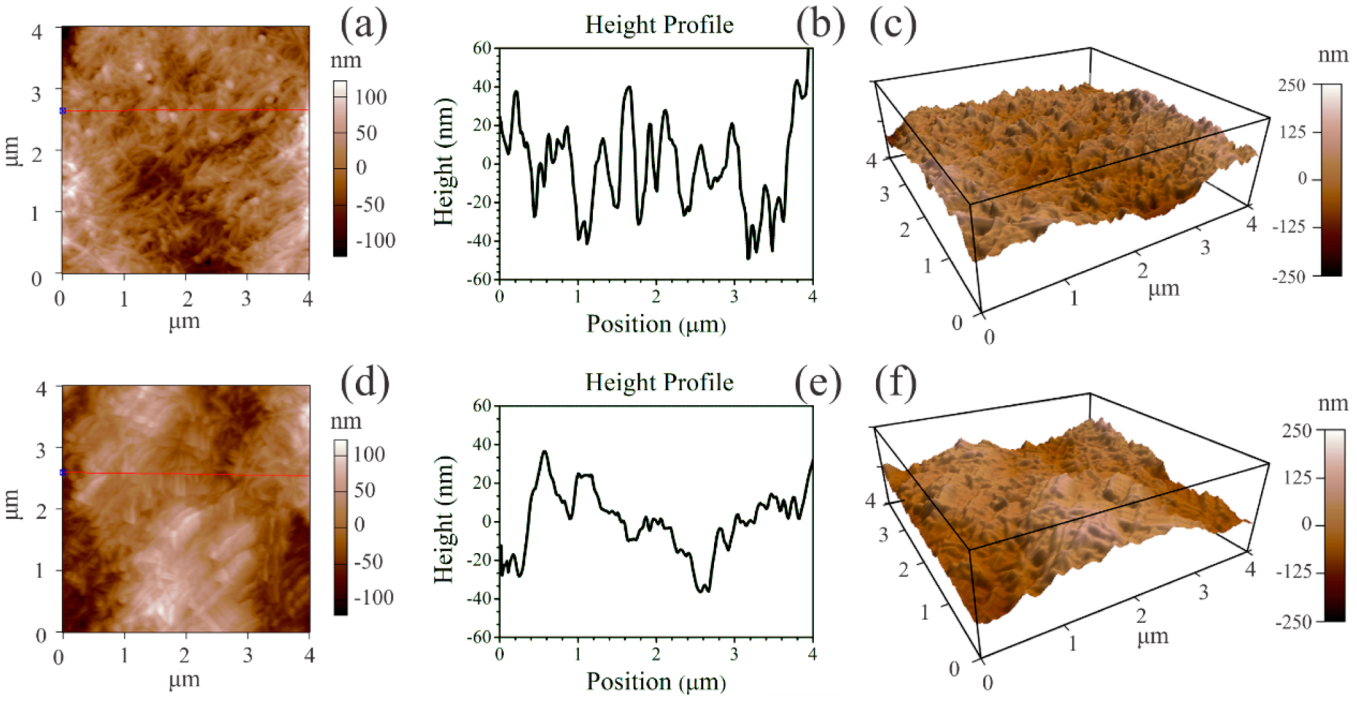

Figure 4. AFM topological images (involving 2D morphology image, height line profile, and 3D AFM topological image) of the (a–c) unpressed and (d–f) after-treated $Cu_{1.75}Te$ NWs/PVDF fabrics.

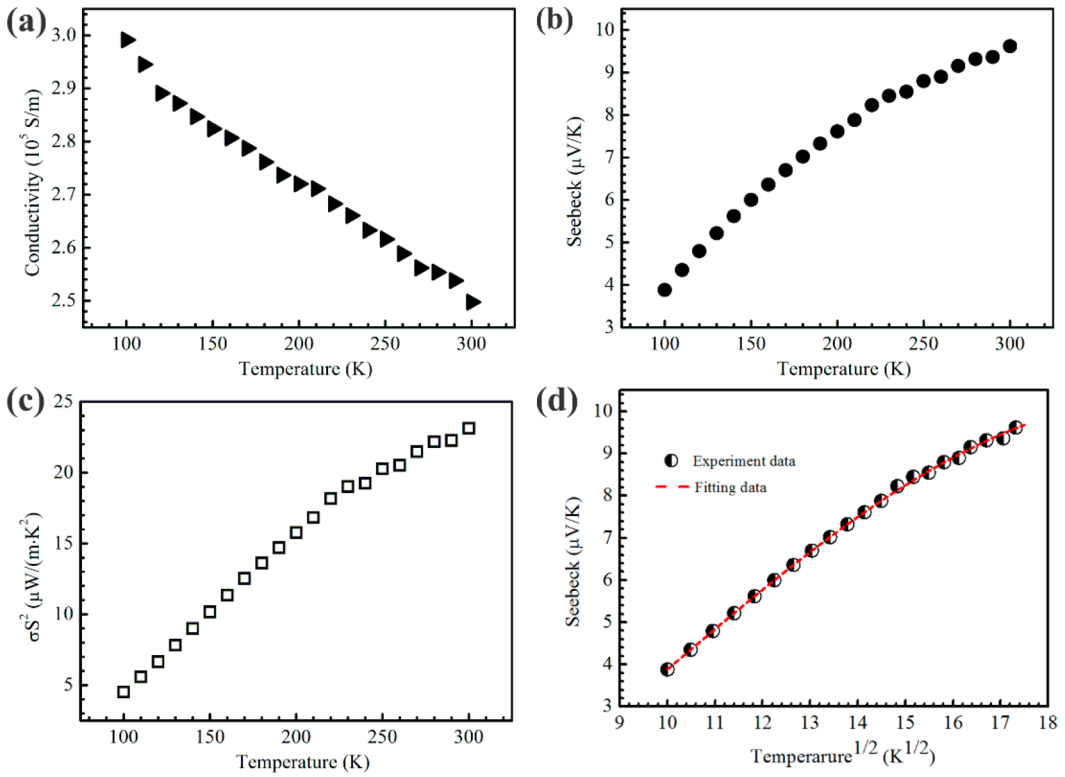

Figure 5. Temperature-dependent (a) electrical conductivity, (b) Seebeck coefficient, and (c) power factor of the thermoelectric $Cu_{1.75}Te$ NWs/PVDF fabric, (d) plot of Seebeck coefficient of the thermoelectric fabric versus $T^{1/2}$.

ficient does not indicate complete metallic-like behavior in spite of the metallic-like temperature-dependent electrical conductivity behavior. Actually, the metallic thermoelectric behavior exhibits linear temperature dependence, but the $Cu_{1.75}Te$ NWs/PVDF fabric presents a slightly decreasing slope with increasing temperature. That is to say, the Seebeck coefficient of $Cu_{1.75}Te$ NW composites exhibits a heterogeneous composite nature with a decreasing Seebeck coefficient with decreased temperature and an increasing slope as the values trend toward zero at lower temperature. This behavior can be ascribed to a heterogeneous model characterized by a linear metallic term plus a modified $T^{1/2}$ exponentially weighted

DOI: 10.1021/acsami.5b07144
ACS Appl. Mater. Interfaces 2015, 7, 21015–21020

semiconducting term, which arises from NW−NW junctions. The model can be described by

$$\alpha(T) = aT + cT^{1/2}\exp\left[-\left(\frac{T_1}{T}\right)^{1/1+d}\right]$$

where T is the absolute temperature, a and c are constants respectively governing the linear and $T^{1/2}$ contributions, T_1 is an energy barrier constant for hopping from NW to NW, and d is the dimensionality of the conducting material. In this case, a dimensionality of 2 demonstrates the low space-filling percolation network of $Cu_{1.75}Te$ NWs. The resulting fitting curve is shown in Figure 5d.

These electrical conductivity and Seebeck coefficient values combine to yield a power factor of $\alpha\sigma^2$ as shown in Figure 5c. Although the Seebeck coefficient value of $Cu_{1.75}Te$ NWs/PVDF fabric is low, the ultrahigh electrical conductivity makes the room-temperature power factor of 23 μW/(mK^2), which is comparable to our previous Bi_2Se_3 nanoplates based flexible film.[1] As thermal conductivity of thin film is difficulty to measure, in order to get an estimated figure of merit (ZT) for the $Cu_{1.75}Te$ NW/PVDF fabric, thermal conductivity of $Cu_{1.75}Te$ NW-based pellet was measured using the laser flash diffusivity apparatus (Netzsch LFA 457) under an argon atmosphere. Here, thermal conductivity is calculated by using the relationship of $\kappa = \rho C_p D$, where ρ is the density, and D and C_p are the thermal diffusivity and the specific heat, respectively. In this case, the average thermal conductivity of $Cu_{1.75}Te$ NW-based pellet was determined around 0.85 W/(mK). However, as phonon scattering with the numerous interfaces and the insulating PVDF is introduced, the lattice thermal conductivity of the present composite fabrics should be significantly decreased and the overall thermal conductivity is believed to be much lower than their bulk/pellets counterpart. Therefore, it is predicted that the real ZT of the composite should be much higher than 0.01 at room temperature. Table 1 compares the

Table 1. Room-Temperature Thermoelectric Performance between the Present $Cu_{1.75}Te$-Based Thermoelectrics Fabrics and Other As-Reported Carbon Related Composite Fabrics

	σ ($\times 10^4$ S/m)	α (μV/K)	PF (μW/mK^2)	ref
$Cu_{1.75}Te$ thin film	65	6	23.4	26
PEDOT:PSS/graphene	15	15	33	28
graphene/PVDF	0.2	18.3	0.52	29
MWCNT/polystyrene	0.5	50	12.5	30
$Cu_{1.75}Te$/PVDF	24.9	9.6	23	this work

room temperature thermoelectric performance between the present $Cu_{1.75}Te$-based thermoelectrics fabrics and the as-reported other related composites, which demonstrates the quite decent thermoelectrical performance of $Cu_{1.75}Te$/PVDF thin film. Moreover, to illustrate the flexibility of the present fabric, the electrical conductivities of $Cu_{1.75}Te$ NWs/PVDF fabric before and after bending tests are exhibited in Figure 6. The electrical conductivities do not vary dramatically until 300 cycles, indicating that the thermoelectric fabric possesses a high flexibility and reliability. During this range, the Seebeck coefficient of the fabric remains almost the same with the increasing bending times, thus the trend for the electrical conductivity represents the variation of power factor. Over all,

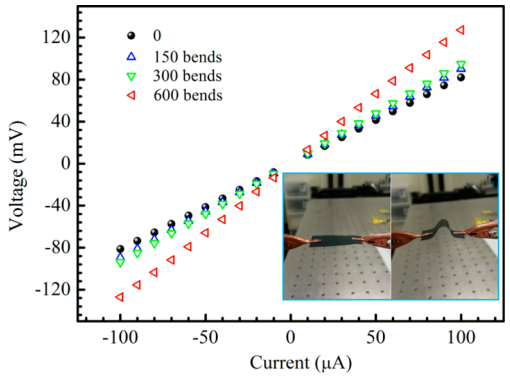

Figure 6. Reliability of a $Cu_{1.75}Te$ NW/PVDF fabric with the inset images for the bending test.

these results demonstrate the feasibility of using the $Cu_{1.75}Te$ NW-based composites in kinetic applications to a certain extent.

In conclusion, a simple and easy to scale-up method to fabricate NW-based flexible thermoelectric fabric is developed and exhibited by using $Cu_{1.75}Te$ NWs as building block and PVDF as flexible substrate. The as-fabricated $Cu_{1.75}Te$ NWs/PVDF fabric exhibits power factor of 23 μW/(m K^2) at room temperature. The thermoelectric properties do not degrade greatly after 300 cycles bending tests. It is believed that the thermoelectric properties of this NW-based thermoelectric fabric can be further improved by using other inorganic NWs, such as Bi_2Te_3, Ag_2Te, or Ag_2Se NWs that having better thermoelectric performance around room temperature.

■ ASSOCIATED CONTENT

Supporting Information

The Supporting Information is available free of charge on the ACS Publications website at DOI: 10.1021/acsami.5b07144.

Detailed synthesis of $Cu_{1.75}Te$ NWs, the fabrication procedure of the nanowire-based flexible thermoelectric, and the experimental setup for thermoelectric measurements (PDF)

■ AUTHOR INFORMATION

Corresponding Authors

*E-mail: zhongqishi@mail.xjtu.edu.cn.
*E-mail: carroldl@wfu.edu.
*E-mail: gwliu76@ujs.edu.cn.

Author Contributions

†C.Z. and C.D. contributed equally to this work.

Notes

The authors declare no competing financial interest.

■ ACKNOWLEDGMENTS

This work was supported by the National Natural Science Foundation of China (51572111), the Program for New Century Excellent Talents in University (NCET-12-0454), Program for Young Excellent Talents in Shaanxi Province (2013KJXX-50), and the Fundamental Research Funds for the Central University (XJJ2015104).

■ REFERENCES

(1) Dun, C.; Hewitt, C.; Huang, H.; Xu, J.; Montgomery, D.; Nie, W.; Jiang, Q.; Carroll, D. L. Layered Bi_2Se_3 Nanoplate/Polyvinylidene

DOI: 10.1021/acsami.5b07144
ACS Appl. Mater. Interfaces 2015, 7, 21015−21020

Fluoride Composite Based n-type Thermoelectric Fabrics. *ACS Appl. Mater. Interfaces* **2015**, *7* (13), 7054−7059.
(2) Dun, C.; Hewitt, C.; Huang, H.; Montgomery, D.; Xu, J.; Carroll, D. Flexible Thermoelectric Fabrics Based on Self-assembled Tellurium Nanorods with a Large Power Factor. *Phys. Chem. Chem. Phys.* **2015**, *17* (14), 8591−8595.
(3) Zhao, W.; Tan, H. T.; Tan, L. P.; Fan, S.; Hng, H. H.; Boey, Y. C. F.; Beloborodov, I.; Yan, Q. N-Type Carbon Nanotubes/silver Telluride Nanohybrid Buckypaper with a High-thermoelectric Figure of Merit. *ACS Appl. Mater. Interfaces* **2014**, *6* (7), 4940−4946.
(4) Zhou, M.; Li, J.-F.; Kita, T. Nanostructured $AgPb_{(m)}SbTe_{(m+2)}$ System bulk Materials with Enhanced Thermoelectric Performance. *J. Am. Chem. Soc.* **2008**, *130* (13), 4527−4532.
(5) Chung, D.; Hogan, T.; Brazis, P.; Rocci-Lane, M.; Kannewurf, C.; Bastea, M.; Uher, C.; Kanatzidis, M. G. $CsBi_4Te_6$: A High-Performance Thermoelectric Material for Low-Temperature Applications. *Science* **2000**, *287* (5455), 1024−1027.
(6) Bubnova, O.; Khan, Z. U.; Malti, A.; Braun, S.; Fahlman, M.; Berggren, M.; Crispin, X. Optimization of the Thermoelectric Figure of Merit in the Conducting Polymer poly(3,4-ethylenedioxythiophene). *Nat. Mater.* **2011**, *10* (6), 429−433.
(7) Tang, D.; Ren, C.; Wang, M.; Wei, X.; Kawamoto, N.; Liu, C.; Bando, Y.; Mitome, M.; Fukata, N.; Golberg, D. Mechanical Properties of Si Nanowires as Revealed by in Situ Transmission Electron Microscopy and Molecular Dynamics Simulations. *Nano Lett.* **2012**, *12*, 1898−1904.
(8) See, K. C.; Feser, J. P.; Chen, C. E.; Majumdar, A.; Urban, J. J.; Segalman, R. a. Water-processable Polymer−nanocrystal Hybrids for Thermoelectrics. *Nano Lett.* **2010**, *10* (11), 4664−4667.
(9) He, M.; Ge, J.; Lin, Z.; Feng, X.; Wang, X.; Lu, H.; Yang, Y.; Qiu, F. Thermopower Enhancement In Conducting Polymer Nanocomposites via Carrier Energy Scattering at the Organic−inorganic Semiconductor Interface. *Energy Environ. Sci.* **2012**, *5* (8), 8351−8358.
(10) Du, Y.; Cai, K. F.; Chen, S.; Cizek, P.; Lin, T. Facile Preparation and Thermoelectric Properties of Bi_2Te_3 Based Alloy Nanosheet/PEDOT: PSS Composite Films. *ACS Appl. Mater. Interfaces* **2014**, *6*, 5735−5743.
(11) Shanker, G. S.; Swarnkar, A.; Chatterjee, A.; Chakraborty, S.; Phukan, M.; Parveen, N.; Biswas, K.; Nag, A. Electronic Grade and Flexible Semiconductor Film Employing Oriented Attachment of Colloidal Ligand-free PbS and PbSe Nanocrystals at Room Temperature. *Nanoscale* **2015**, *7*, 9204−9214.
(12) Finefrock, S. W.; Zhu, X.; Sun, Y.; Wu, Y. Flexible Prototype Thermoelectric Devices Based on Ag_2Te and PEDOT:PSS Coated Nylon Fibre. *Nanoscale* **2015**, *7*, 5598−5602.
(13) Finefrock, S. W.; Wang, Y.; Ferguson, J. B.; Ward, J. V.; Fang, H.; Pfluger, J. E.; Dudis, D. S.; Ruan, X.; Wu, Y. Measurement of Thermal Conductivity of PbTe Nanocrystal Coated Glass Fibers by the 3ω Method. *Nano Lett.* **2013**, *13* (11), 5006−5012.
(14) Harman, T. C.; Taylor, P. J.; Walsh, M. P.; LaForge, B. E. Quantum dot Superlattice Thermoelectric materials and devices. *Science* **2002**, *297* (5590), 2229−2232.
(15) Lin, Z.; Chen, Y.; Yin, A.; He, Q.; Huang, X.; Xu, Y.; Liu, Y.; Zhong, X.; Huang, Y.; Duan, X. Solution Processable Colloidal Nanoplates as Building Blocks for High-Performance Electronic Thin Films on Flexible Substrates. *Nano Lett.* **2014**, *14* (11), 6547−6553.
(16) Li, Z.; Sun, Q.; Yao, X. D.; Zhu, Z. H.; Lu, G. Q. (Max). Semiconductor Nanowires for Thermoelectrics. *J. Mater. Chem.* **2012**, *22* (43), 22821−22831.
(17) Ma, S.; Anderson, K.; Guo, L.; Yousuf, a.; Ellingsworth, E. C.; Vajner, C.; Wang, H.-T.; Szulczewski, G. Temperature Dependent Thermopower and Electrical Conductivityof Te Nanowire/poly(3,4-ethylenedioxythiophene): Poly(4-styrene sulfonate) Microribbons. *Appl. Phys. Lett.* **2014**, *105* (7), 073905.
(18) Luo, M.; Hong, Y.; Yao, W.; Huang, C.; Xu, Q.; Wu, Q. Facile Removal of Polyvinylpyrrolidone (PVP) Adsorbates from Pt Alloy Nanoparticles. *J. Mater. Chem. A* **2015**, *3*, 2770−2775.
(19) Wu, Z.; Chen, Z.; Du, X.; Logan, J. M.; Sippel, J.; Nikolou, M.; Kamaras, K.; Reynolds, J. R.; Tanner, D. B.; Hebard, A. F.; Rinzler, A. G. Transparent,Conductive Carbon Nanotube Films. *Science* **2004**, *816*, 1273−1276.
(20) Moon, G. D.; Ko, S.; Xia, Y.; Jeong, U. Chemical Transformations in Ultrathin nanowires. *ACS Nano* **2010**, *4* (4), 2307−2319.
(21) Jiang, Y.; Xi, J.; Wu, Z.; Dong, H.; Zhao, Z.; Jiao, B.; Hou, X. Highly Transparent, Conductive, Flexible Resin Films Embedded with Silver Nanowires. *Langmuir* **2015**, *31* (17), 4950−4957.
(22) Hu, L.; Kim, H. S.; Lee, J.; Peumans, P.; Cui, Y. Scalable Coating and Properties of Transparent, Flexible, Silver Nanowire Electrodes. *ACS Nano* **2010**, *4* (5), 2955−2963.
(23) Kim, G. T.; Park, J. G.; Lee, J. Y.; Yu, H. Y.; Choi, E. S.; Suh, D. S.; Ha, Y. S.; Park, Y. W. Simple Technique for the Simultaneous Measurements of the Four-probe Resistivity and the Thermoelectric Power. *Rev. Sci. Instrum.* **1998**, *69* (10), 3705−3706.
(24) Kurosaki, K.; Goto, K.; Kosuga, A.; Muta, H.; Yamanaka, S. Thermoelectric and Thermophysical Characteristics of Cu_2Te-Tl_2Te Pseudo Binary System. *Mater. Trans.* **2006**, *47* (6), 1432−1435.
(25) Ballikaya, S.; Chi, H.; Salvador, J. R.; Uher, C. Thermoelectric properties of Ag-doped Cu_2Se and Cu_2Te. *J. Mater. Chem. A* **2013**, *1* (40), 12478−12484.
(26) Mansour, B. A.; Farag, B. S.; Khodier, S. A. Transport properties and band structure of non-stoichiometric $Cu_{2-x}Te$. *Thin Solid Films* **1994**, *247* (1), 112−119.
(27) Tan, L. P.; Sun, T.; Fan, S.; Ng, L. Y.; Suwardi, A.; Yan, Q.; Hng, H. H. Facile Synthesis of Cu_7Te_4 Nanorods and the Enhanced Thermoelectric Properties of Cu_7Te_4−$Bi_{0.4}Sb_{1.6}Te_3$ Nanocomposites. *Nano Energy* **2013**, *2* (1), 4−11.
(28) Xiong, J.; Jiang, F.; Shi, H.; Xu, J.; Liu, C.; Zhou, W.; Jiang, Q.; Zhu, Z.; Hu, Y. Liquid Exfoliated Graphene as Dopant for Improving the Thermoelectric Power Factor of Conductive PEDOT:PSS Nanofilm with Hydrazine Treatment. *ACS Appl. Mater. Interfaces* **2015**, *7* (27), 14917−14925.
(29) Hewitt, C. a.; Kaiser, A. B.; Craps, M.; Czerw, R.; Roth, S.; Carroll, D. L. Temperature Dependent Thermoelectric Properties of Freestanding Few Layer Graphene/Polyvinylidene Fluoride Composite Thin Films. *Synth. Met.* **2013**, *165*, 56−59.
(30) Suemori, K.; Watanabe, Y.; Hoshino, S. Carbon Nanotube Bundles/Polystyrene Composites as High-performance Flexible Thermoelectric Materials. *Appl. Phys. Lett.* **2015**, *106* (11), 113902.

DOI: 10.1021/acsami.5b07144
ACS Appl. Mater. Interfaces 2015, 7, 21015−21020